INVERSE PROBLEM SOLUTION FOR DETERMINING SPACECRAFT ORIENTATION FROM PRESSURE MEASUREMENTS

Jochem Häuser[(1)], Wuye Dai[(1,2)], Georg Koppenwallner[(3)], Jean Muylaert[(4)]

[(1)]Dept. of High Performance Computing and Communications, Center of Logistics and Expert Systems (CLE) GmbH, and University of Applied Sciences, Braunschweig-Wolfenbüttel, Germany Karl-Scharfenberg-Str. 55-57, 38229 Salzgitter, Germany, Email: J.Haeuser@cle.de
[(2)] Aerodynamisches Institut, RWTH Aachen, Wuellnerstr. zw. 5 u. 7,52062 Aachen, Germany Email: w.dai@cle.de
[(3)]HTP Hypersonic Technology Göttingen, Germany, Max-Planck-Str. 19, 37191 Katlenburg-Lindau, *Germany Email:G.Koppenwallner@htg-hst.de*
[(4)]Aerothermodynamics Section, ESA-ESTEC, Noordwijk, The Netherlands, Email: jmuylaer@estec.esa.nl

ABSTRACT

The goal of this paper is to develop a method of predicting the orientation of a blunt-nosed spacecraft(e.g. Kheops Expert) with regard to pitch and sideslip by measuring pressure data at specified locations in the nose region. The strategy devised here is to use analytic sensor functions (ASF) for the prediction of angle of attack (AoA) and yaw angle according to the local pressure data on the vehicle surface. First, the derivation of the sensor functions is presented. In the second step, the range of validity of these formulas is determined with respect to flight velocity (Mach Number), AoA, and yaw angle by employing extensive computer simulation. Third, the corrections of these empirical formulas is devised for the given vehicle so that the required accuracy (resolution better than 0.5 degrees) is guaranteed within the range of the flight envelope. Fourth, the impact of configuration changes on the accuracy of these functions is also evaluated. Results show that this methodology is effective and accurate in the hypersonic regime, provided specific corrections devised from numerical simulation are applied to modify the analytic sensor functions.

1. INTRODUCTION

The ESA-ESTEC proposed air data system is supposed to provide information of the condition on the ambient air and on the flight state of a space vehicle. Therefore, one wishes to relate physical quantities measured at the vehicle surface to atmospheric free stream values as well as to the vehicle's velocity and orientation. Atmospheric free stream values and vehicle flow field determine surface flow values, which can be directly computed using the methods of computational fluid dynamics (CFD). However, for the air data system one has to solve the inverse problem, namely to deduce from surface measurements the state of the atmosphere and the vehicle orientation.

In order to do so, two empirical equations were first developed [Koppenwallner, 2003]. These equations are called analytic sensor functions (ASF) that are based on empirical formulas for which pressure data are obtained from five sensors installed in the nose of the vehicle. Utilizing ASF, both angle of attack (AoA, α) and yaw angle (β) are determined from this pressure distribution.

The next task is to determine the range of validity of these formulas with respect to Mach number as well as AoA and yaw angle. Furthermore, it is expected that numerical computations would allow to provide correction rules for the flight range of interest to improve the accuracy of these formulas, meeting the accuracy requirements of 0.5 degrees for the two angles.

2. ANALYTIC SENSOR FUNCTIONS

ASF determine AoA and yaw angle from vehicle surface pressures, utilizing five pressures at different locations. The form of ASF strongly depends on the five pressure positions. Therefore, it is important to specifically select these positions in order to simplify the form of these functions. Although any set of locations is acceptable for ASF, simple formulas are only obtained for special pressure locations.

For most space vehicles it is acceptable to assume the vehicle nose is axisymmetric. Then the position on the surface can be defined by two angles θ, and ϕ as shown in Fig. 1. Pressure locations are selected according to Fig.1. These locations, with pressures denoted as p_0, p_1, p_2, p_3, and p_4, respectively, are at the stagnation point ($\alpha = 0^o$, $\beta = 0^o$) while the other four locations are given by the following angles: $\theta = 45^o$ and circumference angles ϕ of 0^o, 90^o, 180^o, and 270^o.

Newtonian pressure distribution on axisymmetric bodies was used to derive ASF. The procedure of the derivation is not complex and given in [Koppenwallner, 2003]. Here only the results are listed as Eqs. 1 And 2.

$$\alpha = \tan^{-1}\left(\frac{1}{4\sin^2\pi/4}\frac{(q_3-q_1)}{q_0}\right) \quad (1)$$

$$\beta = \tan^{-1}\left(\frac{\cos\alpha}{4\sin^2\pi/4}\frac{(q_4-q_2)}{q_0}\right) \quad (2)$$

where q is the local pressure difference (with respect to freestream pressure). Hence these measured values can be directly inserted into Eqs.1 and 2.

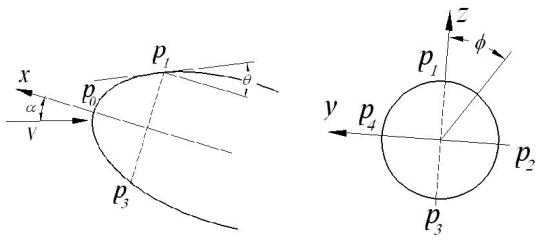

a) Lateral View *(c) Projection against x axis*

Figure 1: Sketch of sensor locations.

3. METHODOLOGY

The ASF (Eqs. 1 and 2) derived above rely on the Newtonian flow assumption for axisymmetric bodies. Since there are stringent requirements on the accuracy of the orientation of the vehicle along its trajectory, namely angles α and β need to be predicted with an error of less than 0.5 degrees, the simple form of Eqs. 1 and 2 needs to be corrected to account for geometrical effects as well as flow viscosity and non-equilibrium phenomena. To this end, the proper flow database has to generated by computer simulation. These data then are used to obtain corrected formulas from Eqs. 1 and 2.

The KHEOPS model (Expert program) proposed by J. Muylaert, ESA and computed by [Walpot, 2002] is the model selected in the present study(referring Fig. 2). This model comprises a body of revolution and an ellipsoid-clothoid-cone, obtained from a two-dimensional longitudinal profile. Its nose, which is of an ellipsoidal shape, has second order smoothness when combined with the cone, to avoid any geometry induced pressure jumps. The grid for KHEOPS, shown in Fig. 3, was generated by GridPro using box technique [Häuser, 2004].

Two solvers were used in the course of the simulations, namely the CFD++ solver from Metacomp, U.S.A. and the ESA Lore code. The CFD++ code is based on a unified grid, unified-physics, and unified-computing framework. CFD++ uses a multi-dimensional second-order total variation diminishing scheme to avoid spurious numerical oscillations in the computed flow field, along with an approximate Riemann (HLLC) solver to guarantee correct signal propagation of convective flow terms. The multi-grid technique is used to accelerate convergence along with a second order accurate point implicit scheme.

The ESA developed Lore code was employed to validate the numerical results obtained from CFD++. The Lore code is a multi-block structured code which covers the subsonic up to hypersonic flow regime. This flow solver is based on a finite volume formulation in which fluxes are computed with a modified AUSM scheme. It incorporates several multi-temperature, finite rate chemistry models. Several algebraic and 2-equation turbulent models are also available. The system of equations is solved fully implicit using a line Gauss-Seidel relaxation method. The Lore code provides an additional feature in form of a boundary condition for a fully catalytic wall, not available in CFD++.

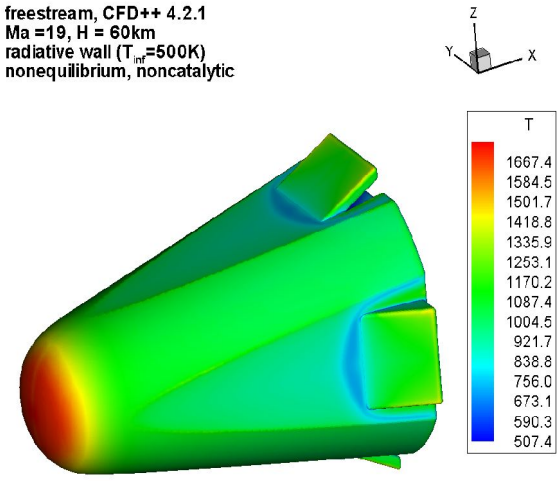

Figure 2: KHEOPS configuration with surface temperature solution

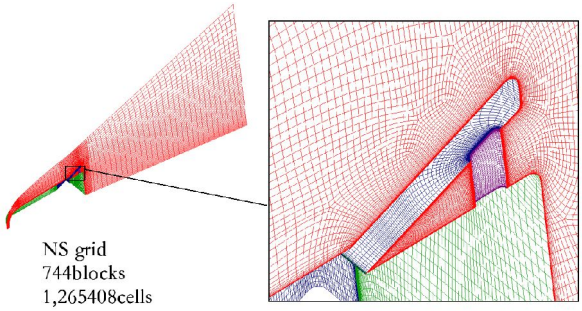

Figure 3 Mesh for the KHEOPS revision 4.2 generated by GridPro using the BOX technique.

A large variety of examples were used to validate the CFD++ code, with validation runs in two- and three-dimensions, using both perfect and real gas, steady flow

and transient flow, inviscid and viscous flow, as well as non-reactive flow and chemically reactive flow[Häuser, 2004] [Chakravarthy, 2002]. The Lore code was also widely used and tested in ESA [Muylaert, 2001]. In the present study, the two solvers were used to solve the same cases and their results were compared. The results obtained from the CFD++ and Lore codes are quite close despite their completely different numerical solution techniques.

The following strategy to study the range of validity of ASF with CFD was used: First, a study of the impact of flow physics (see Sec. 4.1) on the orientation angles at two specified freestream conditions, namely M_∞ = 12.92 and 25.0 was carried out. As a result, it was found that Euler computations were sufficient to achieve the required accuracy. Second, numerous computations were performed at Mach numbers 4.98 and 12.92, investigating effects of angle of attack and yaw angle. Moreover, the influence of freestream Mach number on the analytic sensor functions was studied by varying the Mach number from 1.6 to 25 for angle of attack 10° and yaw angle 5°. Finally, simulating flow past a sphere , the impact of geometry is discussed.

4 RESULTS AND DISCUSSION

4.1. Effects of Flow Models

The flow models considered include

- perfect gas Euler flow (EU),
- perfect gas viscous flow (PG, NS),
- real gas viscous flow with adiabatic wall boundary condition (RG, NS),
- real gas viscous flow with fixed wall temperature (T_w=1,000 K) (RG, NS, TW),
- real gas with chemically reactive, viscous flow with fixed wall temperature (T_w=1,000K) (RG, NS,TW, NE), and
- real gas with chemically reactive, viscous flow with fixed wall temperature (T_w=1,000K) and full catalytic wall (RG, NS, TW, NE, Fullcat).

Most viscous flows in CFD++ are modeled by employing the two-equation k-ε turbulence while in the Lore code the algebraic Baldwin-Lomax model was used. High temperature effects were modeled by the two-temperature chemical non-equilibrium assumption. The reaction model was set up to the standard 5 species and 34 reactions model of Dunn and Kang [Gnoffo,1989].

Effects of different flow models upon pressure coefficient along the wall at Ma =12.92 are shown in Fig. 4. For Ma =15.78 similar results are obtained. Axisymmetric flow simulations were performed, justified by rotational symmetry of the nose and body of KHEOPS, except for the rear part containing the flaps. Neither a difference in the flow model nor a change in the wall boundary condition leads to a significant change in the pressure coefficient.

Heat flux profiles for Ma=25 and α = 10°, β = 5° along different lines along the surface are plotted in Fig. 5. These are results from three dimensional simulations. It is remarkable that both CFD++ and Lore codes provide very close and physically reasonable results.

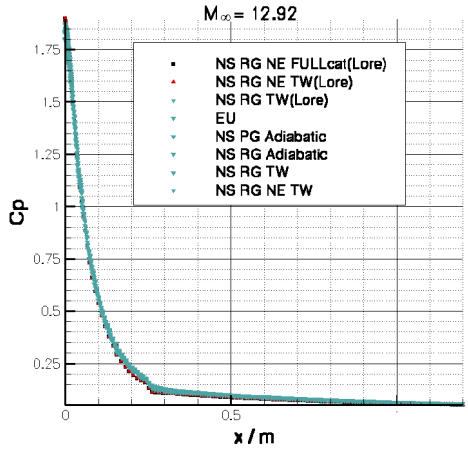

Figure 4: Effect of different flow models upon pressure coefficient along the wall at Ma =12.92.(axis-symmetric simulations, α = 0, β = 0). The results labeled Lore were computed by the Lore code, the others by the CFD++ solver.

The comparisons of absolute errors of the predicted AoA and yaw angle between different flow models and solvers for Ma=12.92 are presented in Figs. 6. Again results from both codes are almost the same. The error of predicted AoA and yaw angle resulting from different flow models, wall boundary conditions, and turbulence models is less than 0.5° , but there is a systematic error. It is concluded that an inviscid flowfield simulation is sufficient to determining the range of validity of ASF.

4.2. Effects of Angle of Attack and Yaw Angle

The predicted AoA using ASF versus actual AoA for different angles of attack and yaw angles are shown in Fig.7. It is observed that the predicted AoA deviates from the actual AoA, but it is interesting to note that the deviation is linear and independent on yaw angle. The deviation between predicted AoA and actual AoA is caused mainly by three factors:

1) The original sensor functions, given in Eqs. 1 and 2, hold for hypersonic flow only, because of the Newtonian flow assumption that leads to a systematic error in the pressure distribution when

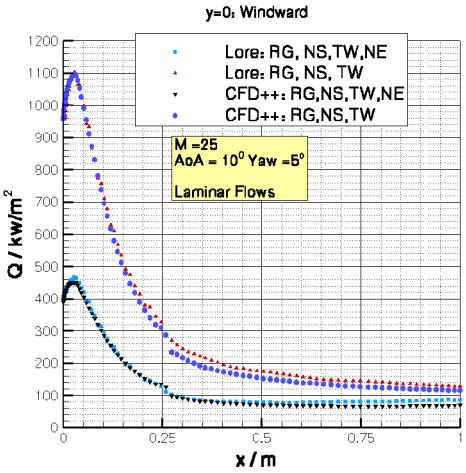

(a) windward side

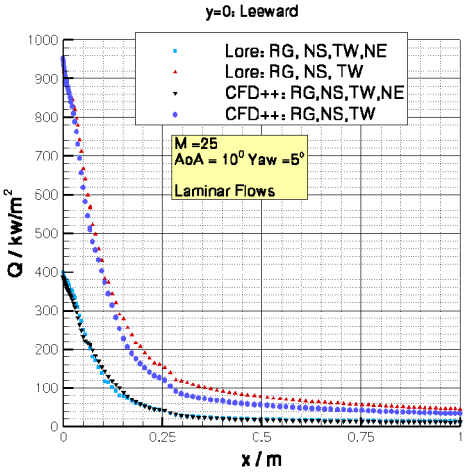

(b) leeward side

Figure 5: Heat flux profiles for Ma=25 (3D Simulation, α = 10° and β = 5°), shown for the (a) windward and (b) side leeward side in the symmetry plane y =0.

compared to the CFD solutions.

2) The geometry studied is that of a three-dimensional vehicle, so axisymmetric flow assumption for ASF causes some error.
3) The CFD method itself also produces numerical errors. Since errors are present, ASF need to be modified accordingly.

Predicted yaw angles are displayed in Fig.8. Like predicted AoAs, the calculated yaw angles deviate from the actual yaw angles. The deviation is approximately linear, but is a function of both AoA and yaw angle. This should be expected from Eq. 2, since the predicted yaw angle is determined by both the pressure relation $\frac{q_4-q_2}{q_0}$ and the predicted AoA.

The requirement is to provide an accuracy in angle

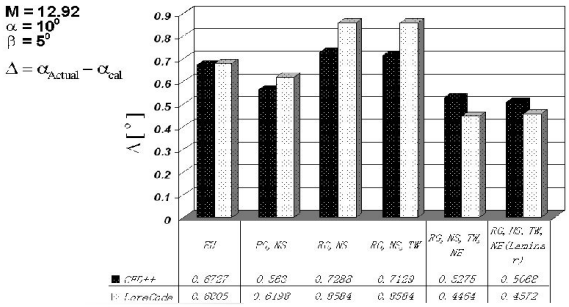

(a) absolute errors of AoA

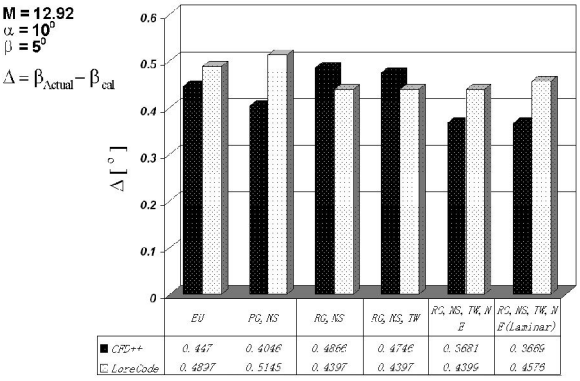

(b) Absolute errors of yaw angle

Figure 6: Comparisons of absolute errors of (a) AoA (b) yaw angle obtained from CFD++ and Lore by employing different flow models for M_∞=12.92, α =10°, β=5°.

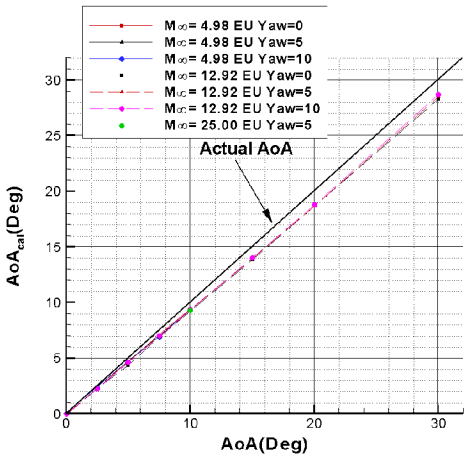

Figure 7: Predicted AoA from surface pressure distribution using ASF versus actual AoA.

resolution better than 0.5 degrees for the complete trajectory. To this end, a simple correction was found, since all errors are linear or approximately linear. The modified results are shown in Figs. 9 and 10 that were obtained using the following modified formulas:

$$\alpha_{modified} = 1.055\,\alpha_{cal} \qquad (3)$$

$$\beta_{modified} = \beta_{cal}(1.07 + 1.04\,\alpha_{cal}^2) \qquad (4)$$

Where the unit of angle is radian, and subscript cal indicates the values got from Eqs.1 and 2.

One can see from Figs. 9 and 10 that as long as $4.98 \leqslant Ma \leqslant 25.0$, $0 < \alpha < 30^o$, and $0 < \beta < 10^o$ the errors in the orientation angles are less than 0.5^o. It should be noticed that the range of validity listed is the range for which computations have been performed, and thus is confirmed to be effective for the sensor functions. In practice, the range of validity could be extended even further.

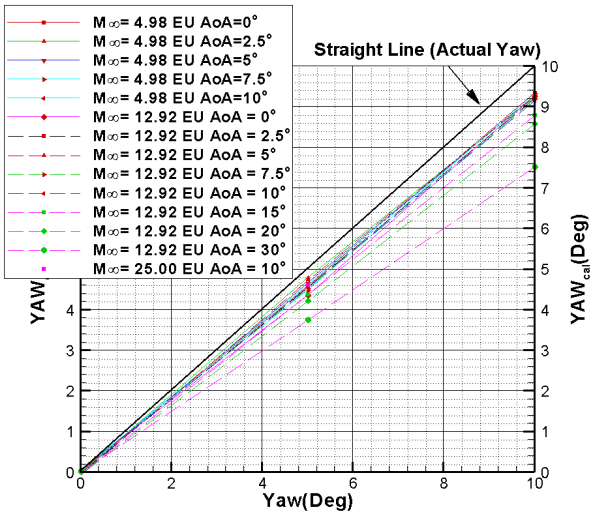

Figure 8: Predicted yaw angle from surface pressure distribution using ASF versus actual Yaw angle.

4.3. Effects of Mach Number

Figure 11 presents the predicted AoA and yaw angle, obtained from the modified formulas Eqs. (3) and (4), versus freestream Mach number for the actual AoA is 10^o and Yaw 5^o. Result shows the sensor functions holds indeed only for Hypersonic flow.

4.4. Impacts of Configuration Changes

From the aforementioned discussion on the factors responsible for the error in angle determination, it can be seen that configuration change gives rise to variation of the error in predicted angles using the original ASF. Substituting a unit sphere for the KHEOPS vehicle, analogous computations were performed to see the effect of configuration changes. Results are compared in Fig 12. Predicted angles for the sphere are more accurate

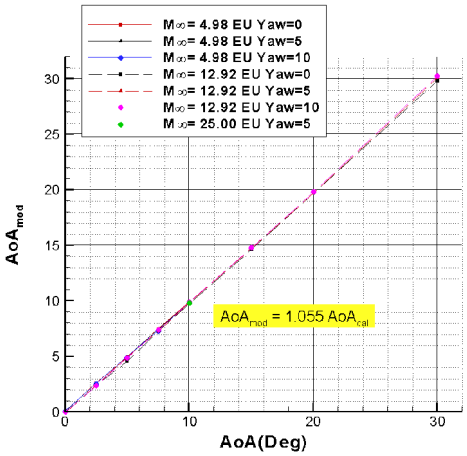

Figure 9: Predicted AoA angle using the correction as stated in Eq. (3).. The modified formula achieves the required precision of 0.5^o.

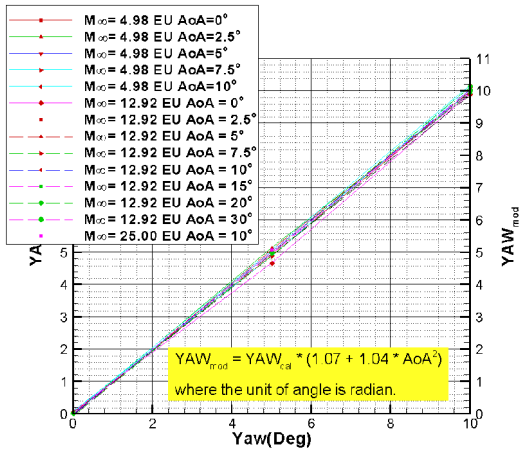

Figure 10: Predicted yaw angle using the correction as stated in Eq.(4). The modified formula achieves the required precision of 0.5^o.

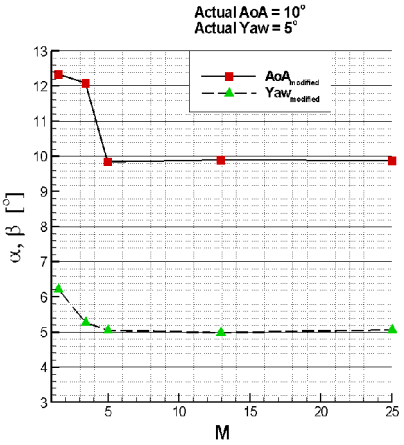

Figure 11: *Variations of modified predicted AoA and Yaw from pressure distribution versus free stream Mach numbers.*

than for KHEOPS. Predicted AoAs almost meet the accuracy requirement without any corrections. This is expected since a sphere is closer to the model from which ASF was obtained. Results indicate that ASF work for different configurations only with proper corrections that depend on the geometry. Hence, corrections Eqs. (3, 4) is not universal applicable, but are valid for KHEOPS only. But it is worth noting that the pressure distribution measured in the nose region of the vehicle accurately predicts its orientation. Therefore, it is the configuration of the nose that matters. The body geometry and the base have little effect.

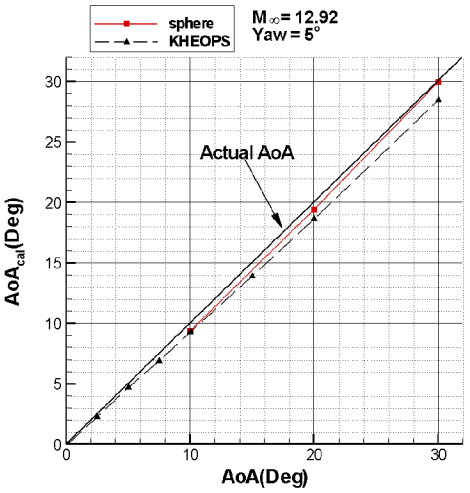

(a) predicted AoA versus Actual AoA

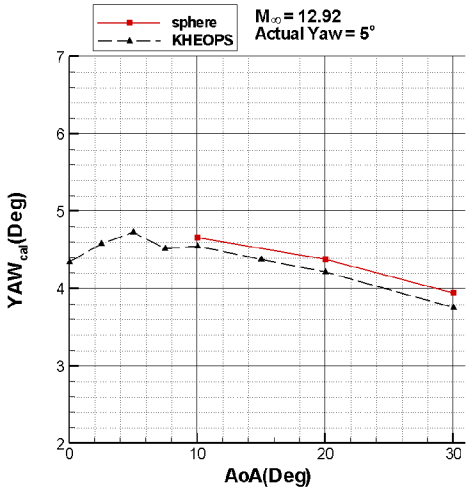

(b) predicted Yaw

Figure 12: Comparisons predicted AoA and Yaw for different of Geometry .

5 CONCLUSIONS

A method of predicting from measuring pressure data at specified locations in the nose region of a space vehicle, its orientation with regard to pitch and sideslip was developed. The strategy is to use ASF for the prediction of AoA and yaw angle using pressure data on specific locations on the vehicle surface. A large number of numerical simulations were performed to study the range of validity of these formulas with regard to flight velocity (Mach Number), AoA, yaw angle, and geometry change. The following conclusions can be drawn: first, the calculated AoA using ASF deviates from the actual AoA and the deviation is almost linear and independent on yaw angle. While, the calculated yaw angle also deviates from the actual yaw angle and the deviation is approximately linear but it is a function of both AoA and yaw angle. Second, Both predicted AoA and yaw angle can be modified using simple corrections to the required precision of 0.5°for the given space vehicle. Third, When $4.98 \leqslant Ma \leqslant 25.0$, $0 < \alpha < 30^{o}$ and $0 < \beta < 10^{o}$, the sensor functions are verified to be effective. In practice, the range of validity could be extended even further. The last, a different nose geometry requires different corrections.

6. REFERENCES

Chakravarthy S., Peroomian O., Goldberg U., Palanishwamy S., and Batten P., *The CFD++ Computation Fluid Dynamics Softerware Suite, MetaComp Technologies,* Inc., Westelake, CA, 2002.

Gnoffo P.A., Gupta R.N., Shinn J,K,; *Conservation Equations and Physical Models for Hypersonic air Flows in Thermal and Chemical Nonequilibrium*, NASA TP 89-2867.1989.

Häuser J. and Dai W., *Numerical simulation for Flush- and Laser Air Data System(FADS).(final report)*, Department of High Performance Computing Center of Logistics and Expert Systems GmbH, Salzgitter, Germany, 2004.

Koppenwallner, G., *Definition of requirements and operational specifications for FADS,* Technical note WP1: Flush and Laser Air Data System, HTG TN-03-6, 2003.

Muylaert J., Kordulla W., Giordano D., Marraffa L., SchwaneR. Spel M., Walpot L., Wong H., *Aerothermodynamic Analysis of Space-Vehicle Phenomena*, Bulletin 105. february 2001.

Walpot, L., Ottens, H., *FESART/EXPERT Aerodynamic and Aerothermodynamic analysis of the REV and KHEOPS configurations*. ESA Technical report, 2002.